

# COMPARISON OF ADSORPTION OF Cd(II) AND Pb(II) IONS ON PURE AND CHEMICALLY MODIFIED FLY ASHES

Eleonora Sočo<sup>\*</sup>, Jan Kalembkiewicz

Rzeszów University of Technology, Faculty of Chemistry, Department of Inorganic and Analytical Chemistry, 6 Powstańców Warszawy Ave., PL-959 Rzeszów, Poland

The study investigates chemical modifications of coal fly ash (FA) treated with HCl or  $\text{NH}_4\text{HCO}_3$  or NaOH or  $\text{Na}_2\text{edta}$ , based on the research conducted to examine the behaviour of Cd(II) and Pb(II) ions adsorbed from water solution on treated fly ash. In laboratory tests, the equilibrium and kinetics were examined applying various temperatures (293 - 333 K) and pH (2 - 11) values. The maximum Cd(II) and Pb(II) ions adsorption capacity obtained at 293 K, pH 9 and mixing time 2 h from the Langmuir model can be grouped in the following order: FA-NaOH > FA- $\text{NH}_4\text{HCO}_3$  > FA > FA- $\text{Na}_2\text{edta}$  > FA-HCl. The morphology of fly ash grains was examined via small-angle X-ray scattering (SAXS) and images of scanning electron microscope (SEM). The adsorption kinetics data were well fitted by a pseudo-second-order rate model but showed a very poor fit for the pseudo-first order model. The intra-particle model also revealed that there are two separate stages in the sorption process, i.e. the external diffusion and the inter-particle diffusion. Thermodynamics parameters such as free energy, enthalpy and entropy were also determined. A laboratory test demonstrated that the modified coal fly ash worked well for the Cd(II) and Pb(II) ion uptake from polluted waters.

**Keywords:** heavy metals, coal fly ash, adsorption, kinetics, thermodynamics

## 1. INTRODUCTION

Adsorption is probably one of the most attractive, simple and efficient processes, and consequently, it is commonly used in industry (Bedoui et al., 2008; Ferreeiraa et al., 2009; Jiang et al., 2010; Rangel-Porras et al., 2010). Although commercially activated carbon, characteristic of high surface areas, porosity and high adsorption capacity can be applied as a potential adsorbent for the removal of heavy metals from industrial wastewater, its use is not recommended because of high operational costs. Thus, there is a growing demand for a low-cost and efficient adsorbent that can be applied to remove heavy metal ions (Ahmaruzzaman, 2010; Cho et al., 2005; Sočo and Kalembkiewicz, 2013).

In recent decades, a number of different solid adsorbents have been considered for their potential usefulness in reducing heavy metals levels in waterways. Some of the adsorbents included clay minerals like bentonite and its pillared forms, iron oxide, red mud, fly ash, and carbonates (Chitrakar et al., 2005; Jiang et al., 2010). While they may have various beneficial applications, the use of any of them has similar disadvantages (Maliyekkal et al., 2010; Reddy et al., 2010; Zhenga et al., 2010).

For example, the performance of iron oxide and red mud in reducing heavy metal concentrations is strongly affected by the solution pH. This has also been demonstrated by other authors (Cho et al., 2005; Debnath and Ghosh, 2009). The key disadvantage of these adsorbents, however, is that the

<sup>\*</sup>Corresponding author, e-mail: eleonora@prz.edu.pl

adsorbed heavy metals can be re-released when the key solution chemical properties such as pH and redox conditions are changed.

The increasing demand for energy throughout the world has led to an increase in the utilisation of coal and, subsequently, in the production of large quantities of fly ash as a waste product (Ruhl et al., 2010). The Rzeszów-Załęże heat and power station is one of the largest power plants in South-Eastern Poland that release coal fly ash (Sočo and Kalembkiewicz, 2007; Sočo and Kalembkiewicz, 2009).

Fly ash is a by-product of coal combustion, partly in the manufacture of pozzolana cement, filler material for reclamation of low lying areas and as well as in the manufacture of fly ash bricks (Canpolat et al., 2004).

In the light of the increasing quantity of fly ash, with a growing demand for electrical energy and hence for thermal power plants, the main challenges faced by the researchers and planners have been to solve the various environmental problems that arise due to the unused and surplus quantity of fly ash (Ahmaruzzaman, 2010).

Although a considerable portion of fly ash is used in industries like construction or soil amendments, there is still a large portion that is directly disposed to the environment. Such disposal is not economic or environmentally sound (Jiao et al., 2011; Seredin and Finkelman, 2008).

Adsorption is an attractive alternative to removing heavy metals from the effluent by using porous materials such as fly ash or zeolite-like substances (Derkowski et al., 2007; Hsu et al., 2008; Penilla et al., 2006).

Fly ash is composed of minerals such as quartz, mullite, subordinately hematite and magnetite, carbon, and a prevalent phase of amorphous aluminosilicate (An and Huang, 2012; Li et al., 2012; Nascimento et al., 2009; Papandreou et al., 2011; Visa et al., 2012).

These oxides are very effective adsorbents. Hence, fly ash (Ahmaruzzaman, 2010; An and Huang, 2012; Nascimento et al., 2009) and its fly ash-derived zeolite (Derkowski et al., 2006; Hsu et al., 2008; Moutsatsou et al., 2006) can be promising candidate materials for removal of heavy metals. The abundance of amorphous aluminosilicate glass, which is the prevalent reactive phase, is what makes fly ash an important source material in the zeolite synthesis. Zeolites are porous materials with a large surface area and cavities of the basket-like frame (Bowman, 2003). Moreover, hydrated aluminosilicate minerals with a three-dimensional open structure making them very useful for solving the mobility of toxic elements in a number of environmental applications are of interest (Jiang et al., 2010; Rangel-Porras et al., 2010). Hence, zeolite has been used for various purposes, e.g., as an adsorbent and ion exchanger in water and wastewater treatment (Scott et al., 2003).

Although several studies on immobilisation of heavy metals by fly ash have been reported, more information is still required to gain better understanding of the relationship between heavy metal sorption properties of fly ashes and their chemical composition (An and Huang, 2012).

Lead and cadmium are the most toxic non-essential heavy metals present in the environment. Lead poisoning in humans causes severe damage to the kidney, nervous system, reproductive system, liver, brain, and may even cause death. Severe exposure to lead has been connected with sterility, abortion, stillbirths and neonatal death (Bedoui et al., 2008). Chronic exposure to elevated level of cadmium is known to cause renal dysfunction (Fanconi syndrome), bone degradation (itai-itai syndrome), cancer, hypertension, liver damage and blood damage (Mathialagan and Viraraghavan, 2002; Ferreira et al., 2009).

As for most adsorption processes in the aqueous phase, any variations in the solution chemistry can lead to changes in other equilibria of the adsorption system. These include changes in the chemistry of

active sites that are responsible for heavy metal ion adsorption, the net charge on the material surface and the nature of the heavy metal species. For example, with an increase in pH, metal ions are hydroxylated. This work was therefore carried out to gain insights into the heavy metal ion uptake by coal fly ash, by studying its physicochemical properties, adsorption kinetics and equilibrium behaviour. The purpose of this research was twofold: firstly, to investigate the effectiveness of FA in reducing heavy metal ion concentrations, and secondly, to gain an insight into the adsorption mechanism of this chemistry-modified coal fly ash product. Importantly, the effect of pH on the adsorption process of heavy metals by FA and FA-modified was explored, and the key physical and chemical characteristics of the product are described.

## 2. EXPERIMENTAL

### 2.1. Apparatus

All reagents were of Fluka or Aldrich analytical grade or of suprapur grade. The elemental composition of the adsorbent and extracts was determined by flame atomic absorption spectroscopy (FAAS; a GBC model of the SavantAA series). Nonmetal (C, N, S) determination in coal fly ash was carried out using the EA 1108 Elemental Analyser (Carbo Erba, Italy). The sample FA was characterised by small-angle X-ray scattering (SAXS) - BRUKER NANOSTAR-U equipped CuK $\alpha$  radiation ( $\lambda = 0.15406$  nm), employing an operating voltage of 50 kV and an intensity of 600  $\mu$ A. SEM images were obtained by scanning with the JEOL JSM-5500LV electron microscope. The spectrum determination of a coal fly ash sample was carried out using a Fourier transform infrared spectrometer (FT-IR; ALPHA model from BRUKER). FT-IR spectrum of the sample was recorded using KBr pellet method. A heating system with a programmable increase of temperature from 25 to 450 °C (DK6 model) and a set of reflux condensers finalised to modify coal fly ash (TMD6 model from VELP, Italy) were also used.

### 2.2. Materials

#### 2.2.1. Adsorbent and characterisation

The coal fly ash sample used in this study was supplied by the Rzeszów-Załęże heat and power station located in South-Eastern Poland. The fly ash under study is a residue of coal combustion utilising pulverised coal firing with the furnace exit gas temperature of 1200 °C. The fly ash moisture content was obtained by drying a 10 - 15 g sample at 105 °C by 24 h. After drying, the sample was placed in a desiccator for a final mass measurement. The pH of the dispersed adsorbent was obtained by adding 2 g of coal fly ash to 100 mL of deionised water. After mixing the dispersion for 15 - 20 min., its pH was measured using a CPI-551 meter.

#### 2.2.2. Spectroscopic measurements (FTIR)

Based on the spectrum obtained from the Fourier transform infrared (FTIR), coal fly ash was analysed as presented in Fig. 1. An absorption broadband in the range of 3400  $\text{cm}^{-1}$ , a band in the range of 1600  $\text{cm}^{-1}$  and an absorption broadband at about 1100  $\text{cm}^{-1}$  were observed in the sample.

The band at 3400  $\text{cm}^{-1}$  was appropriate of  $\nu_{\text{O-H}}$  stretching vibrations. This indicates the presence of both free and hydrogen bonded OH groups on the adsorbent surface. The spectrum was recorded in air atmosphere and the clear-cut interpretation of this band was difficult because it could be derived from –OH groups, chemically bounded with the surface of fly ash, as well as from H-O-H stretching

Table 1. Physical properties of coal fly ash

No.	Determination	Value
1.	pH	8.6
2.	Bulk density, kg m <sup>-3</sup>	620
3.	Moisture content, % (m/m)	1.08
4.	Loss on ignition (LOI)	7.50%
5.	Content of combustible part, % (m/m)	9.9
6.	Specific surface area (m <sup>2</sup> g <sup>-1</sup> )	39.3
7.	Total pore volume (cm <sup>3</sup> g <sup>-1</sup> )	0.171
8.	Average particle size (µm)	22
9.	Content of nonmetals, % (m/m):	
	carbon	5.76
	nitrogen	0.00
	sulfur	0.00
10.	Content of metals oxide, % (m/m):	
	SiO <sub>2</sub>	51
	Al <sub>2</sub> O <sub>3</sub>	20
	Fe <sub>2</sub> O <sub>3</sub>	12.5
	CaO	4
	MgO	2
	K <sub>2</sub> O	0.8
	Na <sub>2</sub> O	0.7
11.	Content of metals, mg kg <sup>-1</sup> :	
	lead	141
	cadmium	4
	chromium	71
	copper	73
	nickel	39
	zinc	98
	manganese	956
	cobalt	29

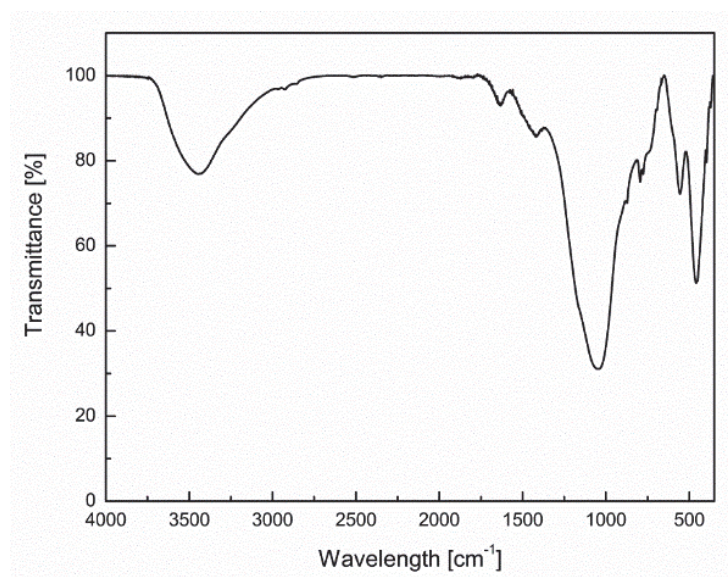


Fig. 1. FTIR spectrum of coal fly ash

vibrations of the water molecule adsorbed (peak at  $3400\text{ cm}^{-1}$ ) on ash surface. The stretching of the OH groups bound to methyl radicals presented a very light signal for FA ( $\sim 2900\text{ cm}^{-1}$ ). The interpretation of the next band ( $1600\text{ cm}^{-1}$ ), was not clear due to its structural complexity but it was found that the band originated from oxide compounds of fly ash derivatives. These compounds influence symmetry of the condensed aromatic rings system, therefore the C=C bond is active in infrared spectra and reveals absorbance at  $1600\text{ cm}^{-1}$ . The IR spectra of the adsorbent indicated weak and broad peaks in the region of  $1600\text{-}1800\text{ cm}^{-1}$  corresponding to the CO group stretching from aldehydes to ketones. The presence of the band at  $1600\text{ cm}^{-1}$  may be due to conjugated hydrocarbon bonded carbonyl groups. The  $1360\text{-}1420\text{ cm}^{-1}$  band in FA may be attributed to the aromatic CH and carboxyl-carbonate structures. The most intense band in the spectrum of coal fly ash is at  $1100\text{ cm}^{-1}$  and can be attributed to the stretching vibrations of the bonds in C-O ( $\nu_{\text{C-O}}$ ) carboxylic, phenolic, etheral groups. The FTIR spectra showed transmittance at  $1100\text{ cm}^{-1}$  due to the vibration of the CO group in lactones.

Moreover, the asymmetrical stretching of the  $\text{TO}_4$  ( $\text{SiO}_4$  or  $\text{AlO}_4$ ) band (broad-strong) corresponds to the variation in frequency ranging from  $1100$  to  $1010\text{ cm}^{-1}$ . The double ring of the secondary building unit (SBU) is observed to be present in FA zeolite structure, corresponding to the infrared frequency equal to  $570\text{ cm}^{-1}$ . Furthermore, there are significantly intense bending modes of the vibration of the Si-O-Al bonds corresponding to  $440\text{ cm}^{-1}$ . Hence, it can be opined that fly ash contains quartz structures. Based on the FTIR spectrum, it can be seen that there are pore openings corresponding to the frequency range of  $450$  to  $400\text{ cm}^{-1}$  in FA which can be attributed to the dissolution of the minerals (viz., quartz and mullite) present in fly ash (Kantiranis et al., 2006). The surface functional groups resulting from IR spectra and the broad bands provide information on the nature of surface oxides. The presence of polar groups on the surface is likely to give considerable cation exchange capacity to the adsorbents. The surface structures of carbon-oxygen (functional groups) are by far the most important elements that influence the surface characteristics and behaviour of coal fly ash.

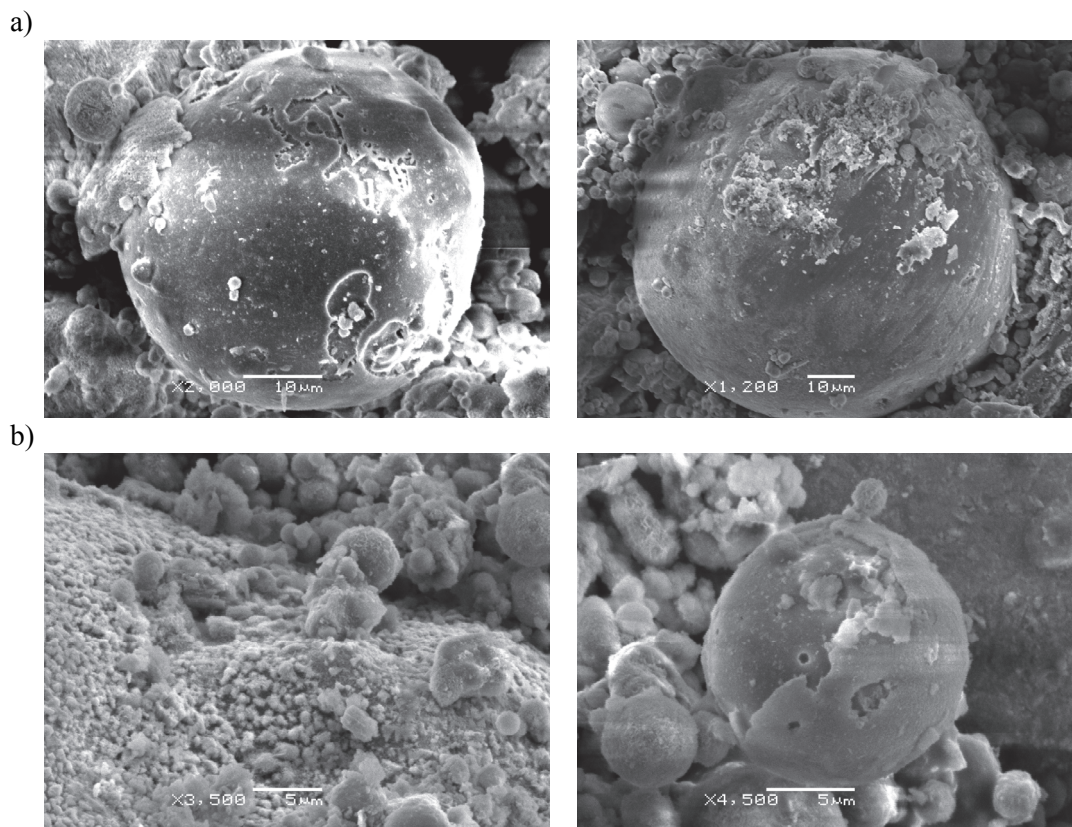


Fig. 2. SEM images of coal fly ash; a) cenospheres, b) plenspheres

### 2.2.3. The pore size distribution plot of coal FA

A scanning electron microscope was used to characterise the morphology of fly ash consisting of cenospheres (Fig. 2a) and plenospheres (Fig. 2b) of different sizes. An idealised structure of FA is shown in Fig. 3. The size of fly ash particles was determined by SAXS. The plot of pore size distribution demonstrated that the majority of pores had a diameter of approximately 28.7 Å (Fig. 4). This indicates that water should be able to diffuse into the structure of the material reasonably well. This fact, together with the relatively small particle size, helped to maximise the exposure of the adsorption sites that participated in the capture of metal ions.

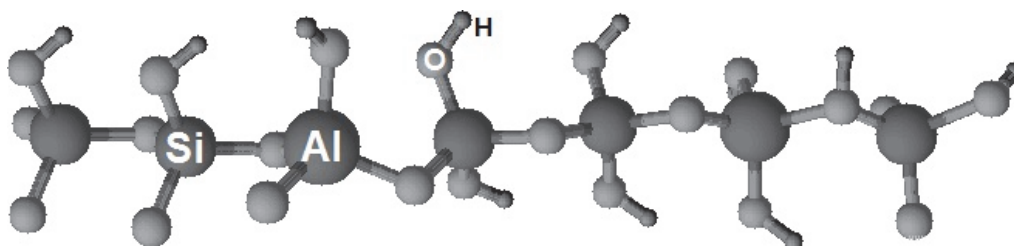


Fig. 3. Idealised structure of FA framework of tetrahedral  $[\text{SiO}_4]^{4-}$  with a Si/Al substitution  $[\text{AlO}_4]^{5-}$

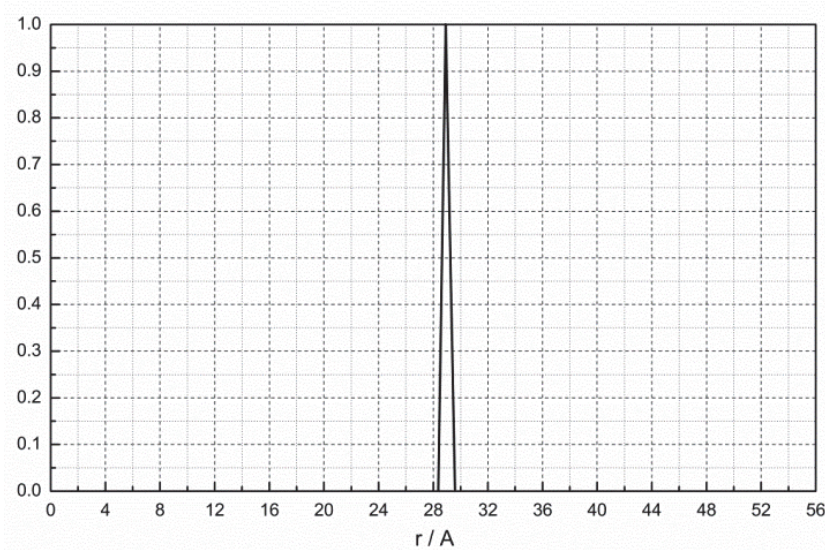


Fig. 4. The pore size distribution plot

## 2.3. Methods

### 2.3.1. Modification of coal fly ash

The sample of coal fly ash was chemically modified by a solution of  $2 \text{ mol}\cdot\text{L}^{-1}$  of NaOH,  $1 \text{ mol}\cdot\text{L}^{-1}$  of HCl,  $1 \text{ mol}\cdot\text{L}^{-1}$  of  $\text{NH}_4\text{HCO}_3$  or  $1 \text{ mol}\cdot\text{L}^{-1}$  of  $\text{Na}_2\text{edta}$ . The modification of the coal fly ash solution at a boiling point was performed as follows: the fly ash was treated with either a  $2 \text{ mol}\cdot\text{L}^{-1}$  solution of NaOH, a  $1 \text{ mol}\cdot\text{L}^{-1}$  solution of HCl, a  $1 \text{ mol}\cdot\text{L}^{-1}$  solution of  $\text{NH}_4\text{HCO}_3$  or in a  $1 \text{ mol}\cdot\text{L}^{-1}$  solution of  $\text{Na}_2\text{edta}$  at a solution to fly ash mass ratio of 10:1 by weight. An adsorbent sample of 20 g mass was placed into a rounded-bottom flask closed with a reflux condenser and was added to a 200 mL solution. The fly ash suspension was then mixed for 6 hours at  $100^\circ\text{C}$ .

After the modification, the adsorbent was decanted and repeatedly distilled in a water bath to obtain the filtrate pH equal to the distilled water pH, and was dried in an electric dryer at a temperature of 105 °C for 24 hours. All laboratory experiments were performed using the adsorbent as received.

### 2.3.2. Adsorption of Cd(II) and Pb(II) ions on coal fly ash

The experiments involving the adsorption with Cd(II) and Pb(II) ions onto modified coal fly ash were conducted by the batch method, which allows for the complete evaluation of the parameters influencing the process of adsorption. In this method, a series of 100 mL glass flasks was filled with a 50 mL metal ion solution of varying concentrations (10-500 mg·L<sup>-1</sup>). Then, 0.5 g of primary-FA/modified-FA nanoparticles were added to each flask and subjected to agitation until equilibrium was attained. The resultant solutions were centrifuged and the supernatant liquids were subjected to the determination of Cd(II) and Pb(II) ions.

The metal ion concentration was analysed by FAAS method. The concentration of metal ions remaining in the solution was calculated by taking the difference of initial and final metal ion concentrations. The adsorbate content in coal fly ash at the adsorption equilibrium  $C_s$  (in mg·g<sup>-1</sup>) and  $A$  (in %) was then obtained by mass balance equation, with  $C_0$  and  $C_{aq}$  (in mg·L<sup>-1</sup>) being the initial and equilibrium metal ion concentrations in the solution,  $V_0$  (in L) the solution volume and  $m$  (in g) the amount of the dry adsorbent used (Kıpçak and Isiyel, 2015).

$$C_s = \frac{(C_0 - C_{aq})V_0}{m} = \frac{C_{ads} V_0}{m} \quad (1)$$

$$A = \frac{(C_0 - C_{aq})}{C_0} 100\% \quad (2)$$

The effect of pH on the extent of metal ion adsorption was investigated by varying the pH in the range of 2-12 for the metal ion concentration of 50 mg·L<sup>-1</sup>. All other experiments were conducted at pH 9 unless otherwise mentioned. The adsorption kinetic experiments were conducted at room temperature using 50 mg·L<sup>-1</sup> of metal ion solutions and 0.5 g of dry FA. The effect of temperature on the degree of adsorption of metal ions on FA was also evaluated for the same concentration of metal ions.

The adsorption isotherms were obtained by adding the modified fly ash (0.5 g) to 50 mL of different concentrations of the metal ion solution (10-500 mg·L<sup>-1</sup>), using Analytical-Reagent Grade salts (AR Grade salts). All samples were placed in an ELPIN-PLUS shaker (type 358 A) at the desired temperature for 2 h. Following this period, some samples were removed from each bottle and filtered, while the heavy metal concentration was analysed by FAAS method in accordance to the standard solution.

The effect of pH on adsorption behaviour was obtained by adjusting the pH of the initial heavy metal solution to the desired pH, using either a 0.1 mol·L<sup>-1</sup> NaOH or a 0.1 mol·L<sup>-1</sup> HNO<sub>3</sub> solution.

The adsorption kinetic experiments were conducted at room temperature using 0.5 g of modified fly ash and 50 mL metal ion solution having a concentration of 50 mg·L<sup>-1</sup>. The solution was mixed at 180 rpm. The rate of heavy metal uptake was then measured by taking samples at various time intervals for five hours.

The effect of temperature on the degree of adsorption of metal ions on modified fly ash was also evaluated for the above- mentioned concentration of metal ion. The uptake rate was determined at 293, 308, 318 and 333 K using deionised water that was adjusted to pH 9. The adsorption set was constructed to allow for the continuous measurement of pH during the mixing phase in the thermostatic system.

#### 2.4. Effect of initial metal ion concentration

The adsorption capacity is dependent on the initial metal ion concentration. The dependence of adsorption capacity of FA on initial concentration of Pb(II) ion at  $20 \pm 2$  °C is shown in Fig. 5. As seen from Fig. 5, the equilibrium uptake increased with an increase in the initial metal ion concentration in the range of the concentrations under study. The higher adsorption capacity connected with the increased initial metal ion concentration is a result of the increase in driving force due to the concentration gradient developed between the bulk solution and the FA surface. Therefore, the values of  $C_s$  increased with the increase of initial metal ion concentrations  $C_0$ .

The heavy metal sorption is attributed to different mechanisms of ion-exchange processes as well as to the adsorption process. During the possible ion exchange process in the beginning, metal ions may move through the pores of FA mass. Secondly, they may replace exchangeable cations, mainly surface hydroxyl groups. The replacement of the surface hydroxyl groups of FA was supported by the experimental results.

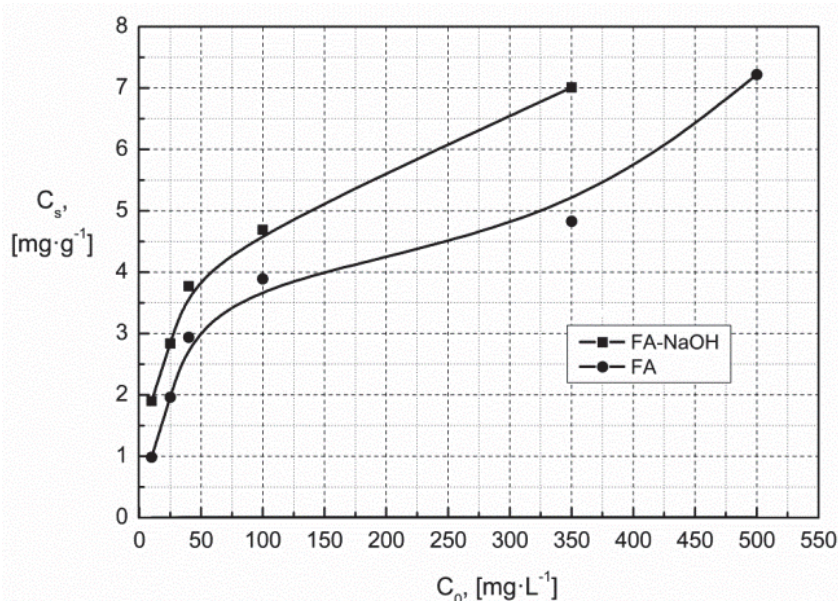


Fig. 5. Effect of initial Pb(II) ion concentration on the adsorption capacity of FA and FA-NaOH

#### 2.5. Effect of pH

One of the most important factors that affect the adsorption of metal ions is the pH of the solution. The pH affects both the adsorbent and adsorbate chemistry in a solution. It was observed from Fig. 6 that the percentage of adsorption of metal ions increased with increase in the solution pH for two metal ions studied. The effect of solution pH on adsorption could be explained by considering the surface charge of FA and the degree of sorbent speciation. Understanding the sorption of metal ions from aqueous solutions on oxides requires knowledge of the chemistry of the oxide/water interface. At acidic pH, the adsorbent surface, the hydrous oxide (MOH) surface will be completely covered by  $\text{H}^+$  ions ( $\text{MOH} + \text{H}^+ \rightarrow \text{MOH}_2^+$ ). At alkaline pH, hydroxide ions react with hydrous oxide to produce deprotonated ( $\text{MOH} + \text{OH}^- \rightarrow \text{MO}^- + \text{H}_2\text{O}$ ). It is well known that both cadmium and lead appear predominantly as  $\text{Cd}^{2+}$  and  $\text{Pb}^{2+}$  at  $\text{pH} < 5$ . As both metal ions exist as  $\text{Cd}^{2+}$  and  $\text{Pb}^{2+}$  at low pH, there will be competition between  $\text{H}^+$  ions for the surface sites and an electrostatic repulsion between the positively charged adsorbent and the adsorbate. At lower pH, the oxide surface was positive in character and there was competition between  $\text{H}^+$  ions and  $\text{M}(\text{II})$  ions for the active surface sites, and hence, lesser adsorption was observed. With an increase in pH from 4 to 6 (at moderate pH), the

surface deprotonation of FA occurs, leading to electrostatic attraction between the positively charged metal ions and the partially negatively charged adsorbent surface, which in turn increases the adsorption percentage. The increase in the adsorption of Cd(II) and Pb(II) on FA with an increase in the solution pH is also explicable on the basis of increased dissociation of surface hydroxyl groups from the surface of FA, while the subsequent formation of metal ions species such as  $\text{CdOH}^+$ ,  $\text{Cd}(\text{OH})_2$ ,  $\text{PbOH}^+$ ,  $\text{Pb}(\text{OH})_2$  and  $\text{Pb}(\text{OH})_4^{2-}$  of low solubility may partly contribute to the maximum percentage removal of metal ions. At the same time, the subsequent formation of metal ion species such as  $\text{CdOH}^+$ ,  $\text{Cd}(\text{OH})_2$ ,  $\text{PbOH}^+$ ,  $\text{Pb}(\text{OH})_2$  or  $\text{Pb}(\text{OH})_4^{2-}$  at pH 8 - 13 of low solubility may contribute to the maximum percentage removal of metal ions ( $\text{CdOH}^+$ ,  $\text{Cd}(\text{OH})_2$ ,  $\text{PbOH}^+$  and  $\text{Pb}(\text{OH})_2$ ) at pH 6-9 or ( $\text{Cd}(\text{OH})_2$ ,  $\text{Pb}(\text{OH})_2$  and  $\text{Pb}(\text{OH})_4^{2-}$ ) at pH > 9 (Figs. 7 and 8). It is well known that lead hydroxide has amphoteric properties. Thus, it appears that as soon as precipitation begins, the adsorption process occurring at the FA surface is overshadowed. Hence, the adsorption observed at pH 6 - 9 is due to the combined process of adsorption ( $\text{CdOH}^+$ ,  $\text{PbOH}^+$ ) and precipitation ( $\text{Cd}(\text{OH})_2$ ,  $\text{Pb}(\text{OH})_2$ ) of metal ions, or at pH > 9, it is also due to the combined process of precipitation ( $\text{Cd}(\text{OH})_2$ ,  $\text{Pb}(\text{OH})_2$ ) and adsorption ( $\text{Pb}(\text{OH})_4^{2-}$ ) of metal ions. In case of Pb(II) ions, it can be seen from Figure 6 that, once the maximum is reached, the percentage adsorption decreases. This trend is attributed to the solubility of formed  $\text{Pb}(\text{OH})_2$  and  $\text{Pb}(\text{OH})_4^{2-}$  at higher pH, whereas, in the case of Cd(II), the percentage adsorption is continued. At lower pH < 3.0, the dissolution of FA may occur and hence, the optimum pH of 9 was selected for the adsorption of Cd(II) and Pb(II) onto FA. The equilibrium adsorption capacity of FA changed within the pH range of 5-7 (Fig. 6) and decreased in solutions with lower pH values. At pH = 2,  $C_\infty$ , it was reduced by 30%, compared with the value at pH 7.

The heavy metal sorption is attributed to different mechanisms of ion-exchange processes as well as to the adsorption process. During the possible ion exchange process, metal ions may in the beginning move through the pores of FA mass. Secondly, they may replace exchangeable cations, mainly surface hydroxyl groups. The replacement of the surface hydroxyl groups of FA was supported by the experimental results.

It was observed that the measured pH was lesser after the equilibration (Fig. 6) compared to that of the initial pH of the solution (Table 1), and hence it was concluded that the adsorption of Cd(II) and Pb(II) onto FA was an ion exchange between the metal cations and the surface protons.

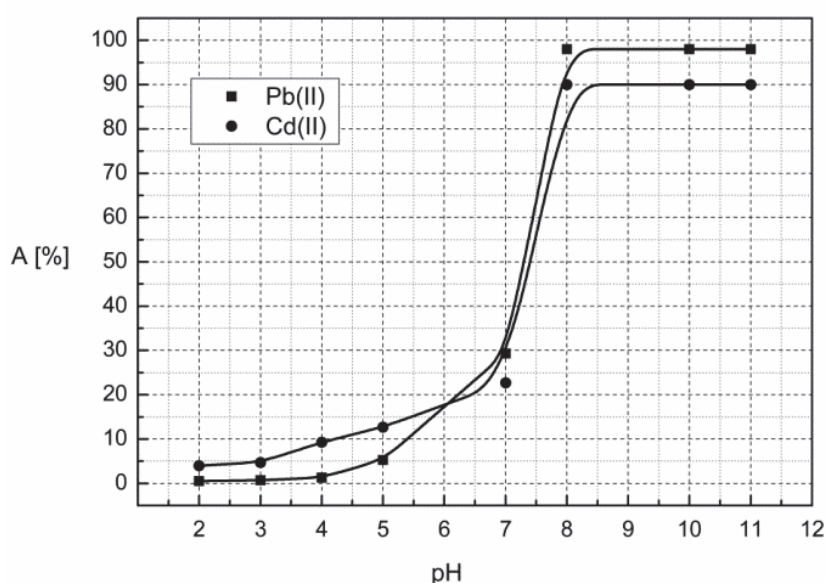


Fig. 6. Effect of the solution pH on the percentage of adsorption of Cd(II) and Pb(II) ions by FA

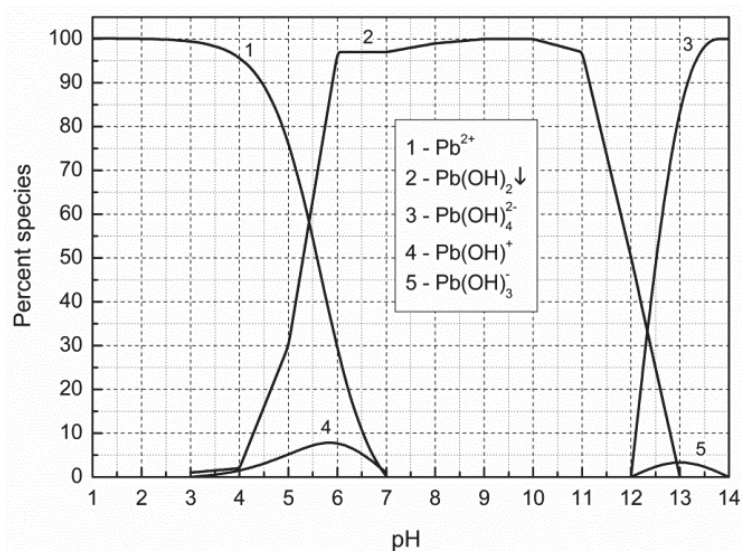


Fig. 7. Lead species as a function of pH (Farooq et al., 2010)

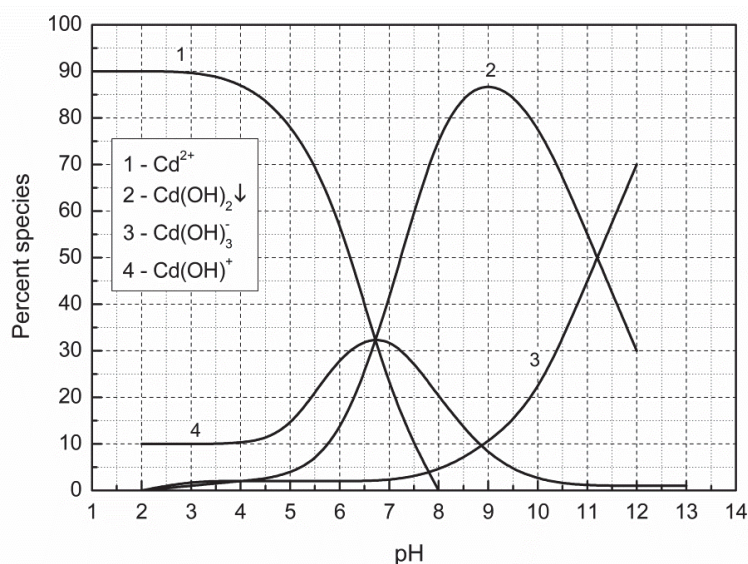


Fig. 8. Cadmium species as a function of pH (Farooq et al., 2010)

## 2.6. Kinetic studies

The influence of mixing time (contact time) on the amount of metal ion remains in the solution after the adsorption by FA was studied on the solution containing  $50 \text{ mg}\cdot\text{L}^{-1}$  of Cd(II) and Pb(II) ions in the range of 15 minutes to 5 hours at room temperature ( $20 \pm 2^\circ\text{C}$ ). It can be seen from Fig. 9 that the amount of Cd(II) and Pb(II) ions remaining in the solution after the adsorption by FA decreased sharply with contact time until the equilibrium was attained. That is the process of adsorption increasing with an increase in contact time until the establishment of equilibrium between the metal ions adsorbed on the surface of FA and those present in the solution. Once the equilibrium was reached, there were no significance changes in metal ion concentrations. The adsorption took place more rapidly in the initial stages and gradually slowed down as it reached the equilibrium state. This behaviour is quite common due to the saturation of the available surface active sites. The metal ion concentration decreased faster within the first 1 h and would decrease to a very low level after 2 hours. The experiments revealed that the equilibrium was reached within 2 hours for both metal ions and after that, saturation could be

expected to occur. However, as can be seen from Figure 9, the rate of adsorption of Pb(II) onto FA surface was faster than that for Cd(II) ions.

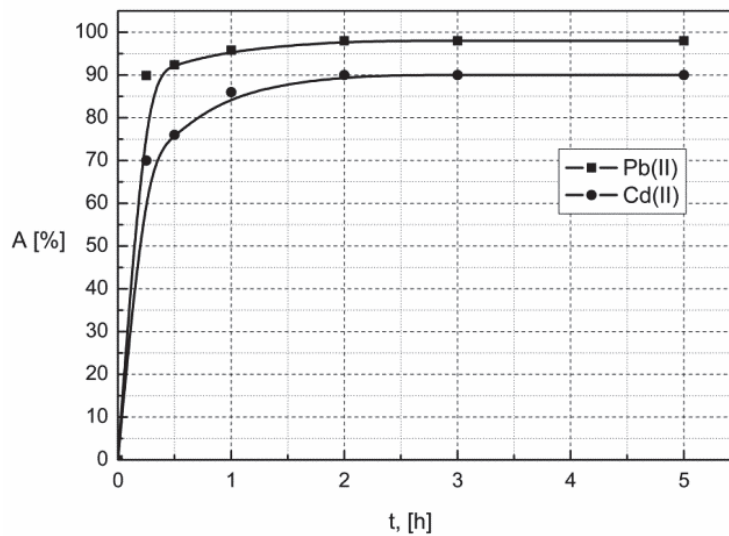


Fig. 9. Mixing time dependence on Cd(II) and Pb(II) ions adsorption (A) on FA

In order to investigate the mechanism and to determine the rate controlling the step of adsorption of Cd(II) and Pb(II) ions, kinetic models were used. The rate constants were calculated using pseudo-first-order and pseudo-second-order kinetic models, whereas the rate controlling step was determined using the intra-particle diffusion model. Table 2 presents the values of these parameters.

The pseudo-first-order model generally can be expressed as follows (Lagergren, 1898):

$$C_s = C_0 (1 - e^{-k_1 t}) \quad (3)$$

$$\ln(C_0 - C_s) = -k_1 t + \ln C_0 \quad (4)$$

$$\ln \frac{C_0}{C_0 - C_s} = k_1 t \quad (5)$$

The values of  $k_1$  were calculated from the slope of the linear plot of  $\ln(C_0 - C_s)$  versus  $t$ . The pseudo-second-order rate model can be determined from the plot of  $1/(C_0 - C_s)$  versus  $t$  using the following formula (Ho and McKay, 1998):

$$\frac{1}{C_0 - C_s} = k_2 t + \frac{1}{C_0} \quad (6)$$

The initial rate of adsorption can be calculated using the following formula:

$$\frac{t}{C_s} = \frac{1}{C_0} t + \frac{1}{k_2 C_0^2} \quad (7)$$

The values of the coefficient of determination  $R^2$  in the pseudo-first-order model not reported in Table 2, were inferior ( $R^2 < 0.6$ ) to those of the pseudo-second-order model, indicating that the pseudo-second-order model is better obeyed than the pseudo-first-order one (Fig. 10).

As part of the kinetic data analysis, it is essential to assess whether the observed data were affected by the diffusion of metal ions into the pore structure of the adsorbent. The rate-limiting step (slowest step of the reaction) may be either the boundary layer (film) or the intra-particle (pore) diffusion of solute on the solid surface from bulk of the solution in a batch process.

Table 2. Kinetic model constants and correlation coefficients for the adsorption systems

Ion	Pseudo-second-order model		Intra-particle diffusion model				
	$k_2$ g/(mg·h)	$R^2$	$k_1$ mg/(g·h <sup>1/2</sup> )	$b$ mg/g	$R^2$	$k_2 \times 10^2$ mg/(g·h <sup>1/2</sup> )	$R^2$
Pb(II)	10.8	1.000	0.6	4.2	1.000	2.4	0.983
Cd(II)	3.6	0.999	1.6	2.7	0.997	3.6	0.997

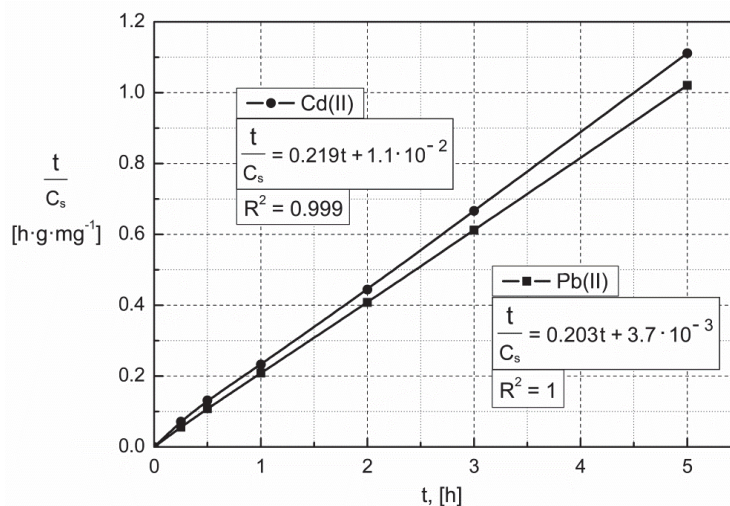


Fig. 10. Kinetics of Cd(II) and Pb(II) ion removal according to the pseudo-second-order

The model is given as follows (Weber and Morris, 1963):

$$C_s = k_2 t^{1/2} + b \quad (8)$$

The values of  $k_{i1}$  and  $k_{i2}$  were computed from the slope of each plot. The value for  $k_{i1}$  was about hundred times greater than that for  $k_{i2}$ , suggesting that the boundary layer (film) diffusion controlled the process of adsorption.

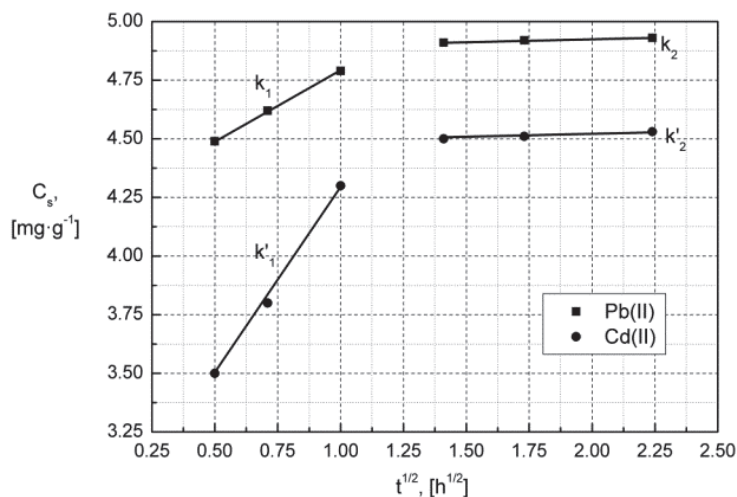


Fig. 11. Intra-particle diffusion model of Cd(II) and Pb(II) ion adsorption by FA

Initially, a linear relationship between  $C_s$  versus  $t^{1/2}$  with a zero intercept was found in both cases, suggesting that the internal diffusion step dominated the adsorption process before the equilibrium was reached. Multi linear plots of  $C_s$  versus  $t^{1/2}$  are presented in Fig. 11. The sharp first linear portion is due

to the boundary layer (film) diffusion, and the second linear one is for the pore diffusion. The  $b$  value for Pb(II) is greater than that for Cd(II) ions, which indicates the greater effect of the boundary layer on the adsorption process of Pb(II).

The Elovich equation, which is applied to heterogeneous surfaces (Chien and Clayton, 1980), was also used for better description of the chemisorption process. It is generally expressed by

$$C_s = \frac{1}{\beta} \ln t + \frac{1}{\beta} \ln \alpha \beta \quad (9)$$

A plot of  $C_s$  versus  $\ln t$  gives a linear trace with a slope of  $1/\beta$  and an intercept of  $1/\beta \ln \alpha \beta$ . Linear plots with reasonable  $R^2$  values indicate agreement with chemisorption processes contributing significantly to adsorption rates. However, experimental data again showed better agreement with the pseudo-second-order kinetic model (Table 2).

The initial adsorption rate  $h$  (Eq. 9), when  $t \rightarrow 0$ , can be calculated using the following formula:

$$h = k_2 C_0^2 \quad (10)$$

The initial rates of adsorption calculated from the pseudo-second-order rate equation for Cd(II) and Pb(II) were 270 and 87.5 [ $\text{mg} \cdot \text{g}^{-1} \cdot \text{h}^{-1}$ ] respectively, indicating the higher adsorption rate of Cd(II) compared to Pb(II) ion on FA.

## 2.7. Equilibrium studies

Isotherms are equilibrium relations between the concentration of adsorbate on the solid phase and its concentration in the liquid phase. Isotherms can be used to obtain the maximum adsorption capacity. Such data provides information on the capacity of the sorbent or the amount required to remove a unit mass of pollutant under system conditions. The data has been subjected to different adsorption isotherms. The Langmuir and Freundlich models are the most common isotherms describing the solid-liquid adsorption system. The adsorption parameters obtained from both models are given in Table 3.

Langmuir isotherm is often used to describe adsorption of solute from liquid solutions and this model assumes monolayer adsorption onto a homogeneous surface with a finite number of identical sites and expressed by the following equation (Langmuir, 1918):

$$C_s = C_\infty \frac{K_L C_{aq}}{1 + K_L C_{aq}} \quad (11)$$

Characteristic constants of Langmuir equation;  $K_L$  related to affinity of the binding sites,  $C_\infty$  Langmuir isotherm constant can be determined from the linearised form:

$$\frac{1}{C_s} = \frac{1}{K_L C_\infty} \cdot \frac{1}{C_{aq}} + \frac{1}{C_\infty} \quad (12)$$

The Freundlich isotherm is an empirical equation employed to describe heterogeneous systems. The Freundlich equation is expressed by (Freundlich, 1906):

$$C_s = K_F (C_{aq})^{1/n} \quad (13)$$

The logarithmic (linearized) form of the Freundlich model is given by the following equation:

$$\log C_s = \frac{1}{n} \log C_{aq} + \log K_F \quad (14)$$

Table 3. The values of isotherm adsorption parameters for Pb(II) ion

Modification	Freundlich				Langmuir		
	$K_F$ $L \cdot mg^{-1}$	$1/n$	$n$	$R^2$	$K_L$ $L \cdot mg^{-1}$	$C_\infty$ $mg \cdot g^{-1}$	$R^2$
NaOH	$3.1 \cdot 10^{-3}$	0.49	2.04	0.988	2.5	21	0.997
NH <sub>4</sub> HCO <sub>3</sub>	$2.6 \cdot 10^{-3}$	0.57	1.75	0.987	0.89	13.8	0.998
primary FA	$2.3 \cdot 10^{-3}$	0.65	1.54	0.991	0.46	8.1	0.996
Na <sub>2</sub> edta	$1.3 \cdot 10^{-3}$	0.83	1.20	0.999	$8.4 \cdot 10^{-2}$	6.5	0.992
HCl	$1.0 \cdot 10^{-3}$	0.81	1.23	0.989	$8.2 \cdot 10^{-2}$	4.9	0.964

From the data it was concluded that the experimental values fitted well into the Langmuir isotherm model (Fig. 12) with high regression coefficients compared to the Freundlich isotherm model (Fig. 13), thus indicating the monolayer adsorption of Cd(II) and Pb(II) ions on the adsorbent surface. To a lesser extent, the equilibrium data was also well described with the Freundlich model, probably due to the true heterogeneous nature of surface sites involved in the process of adsorption. As a result of the scattering of low  $C_{aq}$  data, the Langmuir equation was best used to provide an indication of the equilibrium adsorption capacities rather than the prediction of  $C_s$ , when it was lower than the equilibrium value, even though the  $R^2$  values were high.

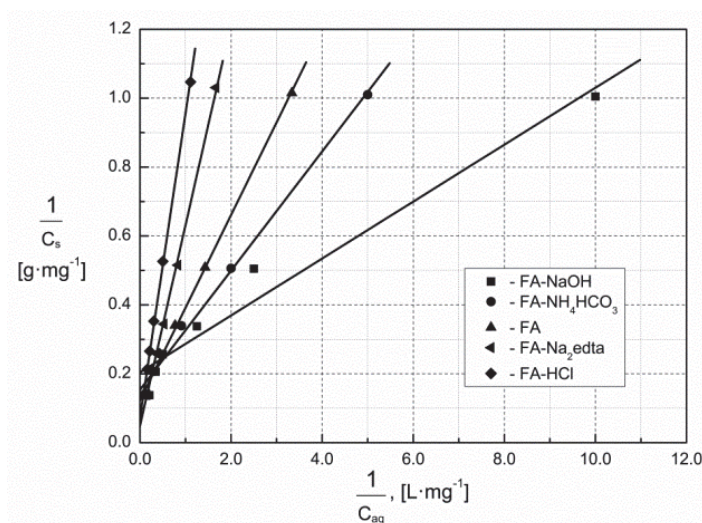


Fig. 12. Langmuir isotherm plot for the adsorption of Pb(II) ions onto primary FA and chemically

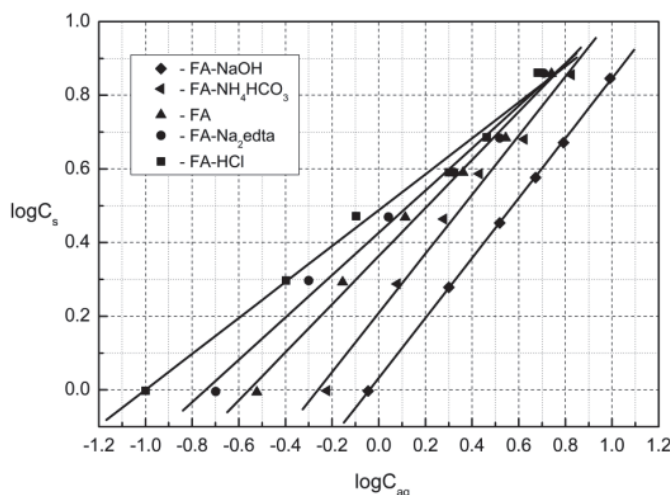


Fig. 13. Freundlich isotherm plot for the adsorption of Pb(II) ion onto primary FA and chemically modified FA

In order to know the feasibility of the isotherm, the essential features of Langmuir model can be expressed in terms of the separation factor or the equilibrium parameter  $R_L$ , which is defined by (Weber and Chakravorti, 1974):

$$R_L = \frac{1}{1 + a_L C_{aq}} \quad (15)$$

$$a_L = \frac{K_L}{C_\infty} \quad (16)$$

Results showed that the sorption of Pb(II) on FA increased as the initial metal ion concentration increased from 10 to 500 mg/L, indicating that the adsorption is even favourable to higher metal ion concentrations that have been investigated. The  $R_L$  values for Pb(II) were in the range of 0.967 to 0.724 for the initial concentration of metal ions (10-500 mg/L). This parameter ( $0 < R_L < 1$ ) indicated that the FA is a suitable adsorbent for the adsorption of Cd(II) and Pb(II) ions from aqueous solutions.

The results obtained on the adsorption of Cd(II) and Pb(II) ions were analysed using the well-known models given by Brunauer, Emmett and Teller (Brunauer et al., 1938). The BET equation is not appropriate for the adsorbent-adsorbate systems. From the data it was concluded that the experimental values fitted well into the Langmuir isotherm model with high regression coefficients compared to the Freundlich isotherm model, thus indicating the monolayer adsorption of Cd(II) and Pb(II) ions onto FA.

### 2.8. Selectivity of FA/modified-FA towards metal ions

The adsorption capacity of FA/modified-FA towards metal ions under study is found to be in the order Pb(II) > Cd(II). The selectivity sequence of metal is generally explained on the basis of properties of metal ions such as ionic radii, atomic weight, softness, electronegativity and hydrolysis constants of metal cations. This selectivity sequence may be explained on the basis of the first hydrolysis constant values for these metal ions. The hydrolysed metal ion ( $\text{MOH}^+$ ) is more strongly sorbed than free metal cations. This can be attributed to the fact that metal ions present in the solution may diffuse to the surface sites slowly or rapidly, although the diffusion might be retarded when metal ions are hydrated. The preferential uptake of Pb(II) ions by FA is assigned to its lowest hydrolysis pH. The uptake of Cd(II) ions is lower compared to Pb(II) ions because of its higher pH values, at which the Cd(II) ion hydrolysis begins to occur. It could be explained by considering the hydrated ionic radii of cations;  $\text{Pb}^{2+}$  (4.01 Å) and  $\text{Cd}^{2+}$  (4.26 Å) - (Kielland, 1937).

Since Pb(II) ions have the smallest hydrated ionic radii, it is possible that with fewer weakly bonded water molecules they tend to move faster to the potential adsorption sites on FA/modified-FA, compared to the cations with higher hydrated ionic radii. This trend could also be accounted for by considering electronegativity. The electronegativity of ions can also play a role in the selectivity of adsorbent towards different heavy metal ions. Since Pb(II) has got the highest electronegativity (1.8), its tendency to react with potential adsorption sites is greater compared to the other metal ions studied.

### 2.9. Thermodynamics studies

The experimental result showed that the adsorption capacity decreases with a drop in the solution temperature (Fig 14).

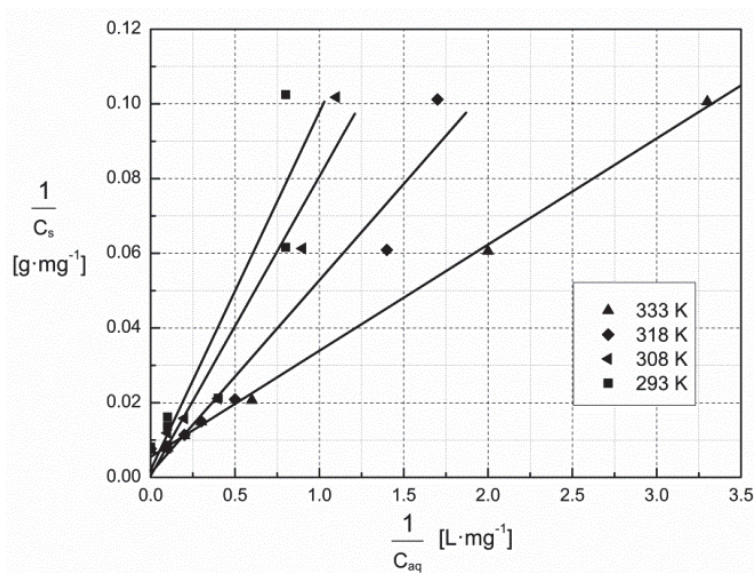


Fig. 14. The effect of temperature on Pb(II) ion adsorption by FA-NaOH; Langmuir isotherm

The decrease in the adsorption rate with the temperature drop may be attributed to the weakening of the adsorptive forces between the active sites of the adsorbents, the adsorbate species and the adjacent molecules of the adsorbed phases.

The variation in the extent of adsorption with respect to temperature has been explained on the basis of thermodynamic parameters, like the change in enthalpy  $\Delta H^0$ , the change in entropy  $\Delta S^0$  and the change in Gibb's free energy  $\Delta G^0$ , were determined using the following Eqs. (17), (18) and (19):

$$\Delta G^0 = -RT \ln K_L \quad (17)$$

$$\Delta H^0 = E_a - RT \quad (18)$$

$$\Delta S^0 = \frac{\Delta H^0 - \Delta G^0}{T} \quad (19)$$

The activation energy  $E_a$  can be calculated using the slope and intercept of the Arrhenius plot of  $\ln K_L$  versus  $1/T$  (Fig. 15).

$$K_L = A \cdot e^{-\frac{E_a}{RT}} \quad (20)$$

$$\ln K_L = -\frac{E_a}{R} \cdot \frac{1}{T} + C \quad (21)$$

Determination of  $E_a$  for Pb(II) and Cd(II) ions was calculated to be 31.6 and 38.5  $\text{kJ} \cdot \text{mol}^{-1}$ , respectively.

The standard free energy change  $\Delta G^0$  reflects the feasibility of the process, while the standard entropy change  $\Delta S^0$  determines the disorderliness of the adsorption at the solid-liquid interface. The values of  $\Delta H^0$  and  $\Delta S^0$  for Pb(II) ion, calculated from the equation, were given as 29.13  $\text{kJ} \cdot \text{mol}^{-1}$  and 90.37  $\text{J} \cdot \text{K}^{-1} \cdot \text{mol}^{-1}$ , respectively. The results are shown in Table 4.

The positive values of the standard enthalpy change  $\Delta H^0$  for the temperature intervals showed the endothermic nature of the adsorption process. The estimated values of  $\Delta H^0$  for the present system were greater than 20  $\text{kJ} \cdot \text{mol}^{-1}$  and hence, the process may have involved a spontaneous sorption mechanism as an ion exchange where chemical bonds are not of strong energies. The positive value of  $\Delta S^0$  suggests that the process of adsorption is spontaneous and thermodynamically favourable. The values of  $\Delta G^0 < 10 \text{ kJ} \cdot \text{mol}^{-1}$  indicate the spontaneous nature of the process.

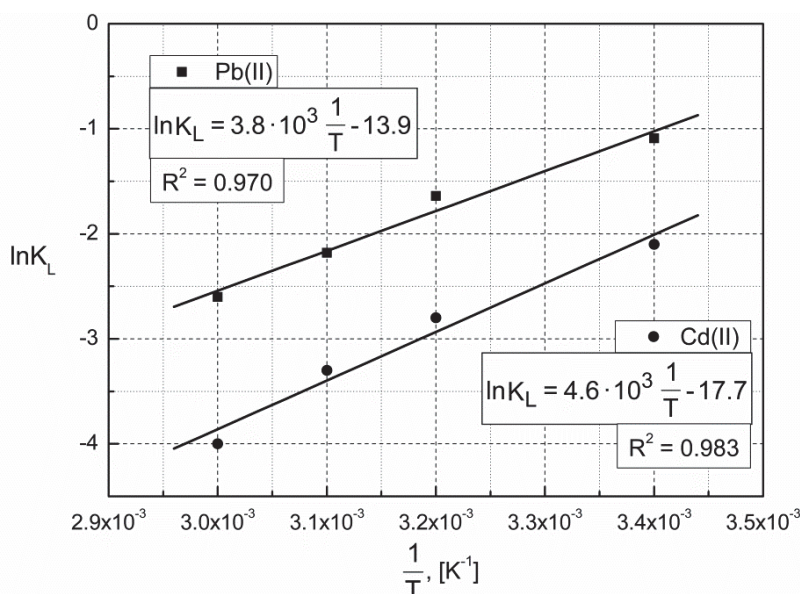


Fig. 15. Arrhenius plot for the adsorption of Cd(II) and Pb(II) ions by FA-NaOH

Table 4. The characteristic parameters of adsorption process of Pb(II) and Cd(II) ions on FA-NaOH

Ion	Temperature K	Langmuir constants			Freundlich constants				$\Delta G^0$ kJ/mol	$\Delta H^0$ kJ/mol	$\Delta S^0$ J/(K·mol)
		$C_\infty$ mg/g	$K_L$ L/g	$R^2$	1/n	n	$K_F$ L/g	$R^2$			
Pb(II)	293	10.6	0.34	0.982	0.99	1.01	8.22	0.821	2.66	29.13	90.37
	308	181.8	0.19	0.998	1.13	0.88	9.98	0.902	4.20		
	318	204.1	0.11	0.987	1.09	0.92	16.33	0.937	5.67		
	333	312.5	0.07	0.988	0.84	1.19	25.74	0.977	7.20		
Cd(II)	293	5.1	0.12	0.978	1.06	0.94	5.50	0.906	5.12	36.05	105.56
	308	35.3	0.06	0.996	0.90	1.11	7.23	0.896	7.17		
	318	126.8	0.04	0.993	0.96	1.04	10.11	0.900	8.59		
	333	205.4	0.02	0.989	0.85	1.18	18.34	0.887	11.07		

### 3. CONCLUSIONS

The results show that NaOH-treated fly ash (FA-NaOH) is a more effective adsorbent than HCl-treated fly ash (FA-HCl) or untreated fly ash (FA). The pH of the solution, the initial metal ion concentration, the time and temperature are found to play a crucial role in the process of adsorption of Pb(II) and Cd(II) ions onto the FA/modified-FA. Results suggest that treating fly ash with an alkaline solution was a promising way to enhance the inhibition of heavy metal mobility. The Langmuir and Freundlich isotherms were used to fit the experimental equilibrium data. Both isotherms provide accurate representation over the range of experimental conditions, though the Langmuir model performs slightly better with high regression coefficients. The maximum monolayer adsorption capacity of the FA-NaOH was unaffected at 333 K, 2 hours and pH 9, but decreased at lower pHs, and was found to be 205 and 312 mg·g<sup>-1</sup> for Cd(II) and Pb(II) ions respectively. Kinetic studies demonstrated that the mechanism for adsorption of metal ions followed the pseudo-second-order rate model, providing the best fit for the experimental data. The intra-particle diffusion model suggested that the initial adsorption rate was controlled by the film diffusion, which was followed by the pore diffusion or the external mass transfer effects. The thermodynamic calculations (heat of adsorption -  $\Delta H^0$ ) suggested that the adsorption of Cd(II) and Pb(II) ions onto FA-NaOH is the endothermic nature of the process, whereas the low values

of free energy ( $\Delta G^0$ ) indicated the spontaneity of the process. The equilibrium experiments show that the selectivity of FA and FA-NaOH towards Pb(II) ions is higher than that of Cd(II) ions, which is related to their hydrated ionic radius and the first hydrolysis equilibrium constant. The competitive adsorption experiment indicated that FA and FA-NaOH had a stronger affinity to Pb(II) than to Cd(II) ion. Based on the adsorption capacity obtained, a conclusion can be made that FA-NaOH can be used to treat wastewaters containing heavy metal ions.

*The X-ray analysis was carried out in the Laboratory of Spectrometry, Faculty of Chemistry, Rzeszów University of Technology, 6 Powstańców Warszawy Ave., 35-959 Rzeszów, Poland and was financed from the DS budget.*

*The SEM analysis was carried out in the Laboratory of Scanning Microscopy, Faculty of Civil and Environmental Engineering, Department of Materials Engineering and Building Technology, Rzeszów University of Technology, 6 Powstańców Warszawy Ave., 35-959 Rzeszów, Poland and was financed from DS budget.*

## SYMBOLS

$A$	adsorption percentage, %
$b$	film thickness, $\text{mg}\cdot\text{g}^{-1}$
$C_0$	initial concentration of adsorbate in the solution, $\text{mg}\cdot\text{L}^{-1}$ or ppm
$C_{aq}$	unadsorbed concentration of the component in an aqueous solution at the adsorption equilibrium, $\text{mg}\cdot\text{L}^{-1}$ or ppm
$C_{ads}$	adsorbed concentration of the component from an aqueous solution at the adsorption equilibrium ( $C_{ads} = C_0 - C_{aq}$ ), $\text{mg}\cdot\text{L}^{-1}$ or ppm
$C_s$	equilibrium solid-phase content, $\text{mg}\cdot\text{g}^{-1}$
$C_\infty$	maximum content of adsorbate in ash at the adsorption equilibrium, $\text{mg}\cdot\text{g}^{-1}$
$E_a$	activation energy, $\text{kJ}\cdot\text{mol}^{-1}$
$\Delta G^0$	free energy change of the adsorption process, $\text{kJ}\cdot\text{mol}^{-1}$
$\Delta H^0$	enthalpy change of the adsorption process, $\text{kJ}\cdot\text{mol}^{-1}$
$h$	initial adsorption rate, $\text{mg}\cdot\text{g}^{-1}\cdot\text{h}^{-1}$
$K_F$	Freundlich adsorption coefficient, $\text{L}\cdot\text{g}^{-1}$
$k_1$	first order rate constant, $\text{h}^{-1}$
$k_2$	second order rate constant, $\text{g}\cdot\text{mg}^{-1}\cdot\text{h}^{-1}$
$k_i$	intra-particle diffusion rate constant, $\text{mg}\cdot\text{g}^{-1}\cdot\text{h}^{-1/2}$
$LOI$	loss on ignition, %
$m$	adsorbent mass (coal fly ash), g
$n$	Freundlich heterogeneity factor for each component
$R_L$	separation factor
$R$	universal gas constant ( $8.314 \text{ J}\cdot\text{K}^{-1}\cdot\text{mol}^{-1}$ )
$R^2$	linear regression coefficient
$\Delta S^0$	entropy change of the adsorption process, $\text{J}\cdot\text{K}^{-1}\cdot\text{mol}^{-1}$
$V_0$	initial volume of the aqueous phase under adsorption, mL or L
$T$	absolute temperature, K
$t$	adsorption time, h

### Greek symbols

$\alpha$	initial adsorption rate, $\text{mg}\cdot\text{g}^{-1}\cdot\text{h}^{-1}$
$\beta$	adsorption rate related to the extent of surface coverage and the activation energy for chemisorption, $\text{g}^{-1}\cdot\text{mg}$

## REFERENCES

- Ahmaruzzaman M., 2010. A review on the utilization of fly ash. *Prog. Energ. Combust.*, 36, 327-363. DOI: 10.1016/j.peccs.2009.11.003.
- An C., Huang G., 2012. Stepwise adsorption of phenanthrene at the fly ash-water interface as affected by solution chemistry: Experimental and modeling studies. *Environ. Sci. Technol.*, 46, 12742-12750. DOI: 10.1021/es3035158.
- Bedoui K., Bekri Abbes I., Srasra E., 2008. Removal of cadmium(II) from aqueous solution using pure smectite and Lewatite S 100: The effect of time and metal concentration. *Desalination*, 223, 269-273. DOI: 10.1016/j.desal.2007.02.078.
- Bowman R.S., 2003. Applications of surfactant-modified zeolites to environmental remediation. *Micropor. Mesopor. Mat.*, 61, 43-56. DOI: 10.1016/S1387-1811(03)00354-8.
- Brunauer S., Emmett P.H., Teller E., 1938. Adsorption of gases in multimolecular layers. *J. Am. Chem. Soc.* 60, 309-319. DOI: 10.1021/ja01269a023.
- Canpolat F., Yilmaz K., Kose M.M., Sumer M., Yurdusev M.A., 2004. Use of zeolite, coal bottom ash and fly ash as replacement materials in cement production. *Cement Concrete Res.*, 34, 731-735. DOI: 10.1016/S0008-8846(03)00063-2.
- Chien S. H., Clayton W. R., 1980. Application of Elovich equation to the kinetics of phosphate release and sorption in soils. *Soil Sci. Soc. Am. J.*, 44, 265-268. DOI: 10.2136/sssaj1980.03615995004400020013x.
- Chitrakar R., Tezuka S., Sonoda A., Sakane K., Ooi K., Hirotsu T., 2005. Adsorption of phosphate from seawater on calcined MgMn-layered double hydroxides. *J. Colloid Interf. Sci.*, 290, 45-51. DOI: 10.1016/j.jcis.2005.04.025.
- Cho H., Oh D., Kim K., 2005. A study on removal characteristics of heavy metals from aqueous solution by fly ash. *J. Hazard. Mater.*, 127, 187-195. DOI: 10.1016/j.jhazmat.2005.07.019.
- Debnath S., Ghosh U.C., 2009. Nanostructured hydrous titanium(IV) oxide: synthesis characterization and Ni(II) adsorption behavior. *Chem. Eng. J.*, 152, 480-491. DOI: 10.1016/j.cej.2009.05.021.
- Derkowski A., Franus W., Beran E., Czimerová A., 2006. Properties and potential applications of zeolitic materials produced from fly ash using simple method of synthesis. *Powder Technol.*, 166, 47-54. DOI: 10.1016/j.powtec.2006.05.004.
- Derkowski A., Franus W., Waniak-Nowicka H., Czimerová A., 2007. Textural properties vs. CEC and EGME retention of Na-X zeolite prepared from fly ash at room temperature. *Int. J. Miner. Process.*, 82, 57-68. DOI: 10.1016/j.minpro.2006.10.001.
- Farooq U., Kozinski J.A., Khan M.A., Athar M., 2010. Biosorption of heavy metal ions using wheat based biosorbents - A review of the recent literature. *Bioresource Technol.*, 101, 5043-5053. DOI: 10.1016/j.biortech.2010.02.030.
- Ferreira T.R., Lopes C.B., Litoa P.F., Oterob M., Lina Z., Rochaa J., Pereirab E., Silvaa C.M., Duarteb A., 2009. Cadmium(II) removal from aqueous solution using microporous titanasilicate ETS-4. *Chem. Eng. J.*, 147, 173-179. DOI: 10.1016/j.cej.2008.06.032.
- Freundlich H.M.F., 1906. Über die adsorption in lösungen. *J. Phys. Chem.* 57, 385-470.
- Ho Y. S., McKay G., 1998. Sorption of dye from aqueous solution by peat. *Chem. Eng. J.*, 70, 115-124. DOI: 10.1016/S0923-0467(98)00076-1.
- Hsu T.-C., Yu C.-C., Yeh C.-M., 2008. Adsorption of Cu<sup>2+</sup> from water using raw and modified coal fly ashes. *Fuel*, 87, 1355-1359. DOI: 10.1016/j.fuel.2007.05.055.
- Jiang M., Jin X., Lu X., Chen Z., 2010. Adsorption of Pb(II), Cd(II), Ni(II) and Cu(II) onto natural kaolinite clay. *Desalination*, 252, 33-39. DOI: 10.1016/j.desal.2009.11.005.
- Jiao F., Wijaya N., Zhang L., Ninomiya Y., Hocking R., 2011. Synchrotron-Based XANES Speciation of Chromium in the Oxy-Fuel Fly Ash Collected from Lab-Scale Drop-Tube Furnace. *Environ. Sci. Technol.*, 45, 6640-6646. DOI: 10.1021/es200545e.
- Kantiranis N., Filippidis A., Mouhtaros T., Paraskevopoulos K.M., Zorba T., Squires C., Charistos D., 2006. EPI-type zeolite synthesis from Greek sulphocalcic fly ashes promoted by H<sub>2</sub>O<sub>2</sub> solutions. *Fuel*, 85, 360-366. DOI: 10.1016/j.fuel.2005.07.015.
- Kıpçak İ., İsiyel T. G., 2015. Magnesite tailing as low-cost adsorbent for the removal of copper(II) ions from aqueous solution. *Korean J. Chem. Eng.*, 32(8), 1634-1641. DOI: 10.1007/s11814-014-0377-8.

- Lagergren S., 1898. Zur theorie der sogenannten adsorption gel'ster stoffe. *Kungliga Svenska Vetenskapsakademines, Handlingar*, 24(4), 1-39.
- Langmuir I., 1918. The adsorption of gases on plane surfaces of glass, mica and platinum. *J. Am. Chem. Soc.* 40, 1361-1403. DOI: 10.1021/ja02242a004.
- Li H-Q., Huang G-H., An Ch-J., Zhang W-X., 2012. Kinetic and equilibrium studies on the adsorption of calcium lignosulfonate from aqueous solution by coal fly ash. *Chem. Eng. J.*, 200-202, 275-282. DOI: 10.1016/j.cej.2012.06.051.
- Maliyekkal S.M., Anshup, Antony K.R., Pradeep T., 2010. High yield combustion synthesis of nanomagnesia and its application for fluoride removal. *Sci. Tot. Environ.*, 408, 2273-2282. DOI: 10.1016/j.scitotenv.2010.01.062.
- Mathialagan T., Viraraghavan T., 2002. Adsorption of Cd from aqueous solutions by perlite. *J. Hazard. Mater.*, 94, 291-303. DOI: 10.1016/S0304-3894(02)00084-5.
- Moutsatsou A., Stamatakis E., Hatzizotzia K., Protonotarios V., 2006. The utilization of Ca-rich and Ca-Si-rich fly ashes in zeolites production. *Fuel*, 85, 657-63. DOI: 10.1016/j.fuel.2005.09.008.
- Nascimento M., Moreira Soares P.S., de Souza V.P., 2009. Adsorption of heavy metal cations using coal fly ash modified by hydrothermal method. *Fuel*, 88, 1714-1719. DOI: 10.1016/j.fuel.2009.01.007.
- Papandreou A.D., Stournaras C.J., Pnias D., Paspaliaris I., 2011. Adsorption of Pb(II), Zn(II) and Cr(III) on coal fly ash porous pellets. *Miner. Eng.*, 24, 1495-1501. DOI: 10.1016/j.mineng.2011.07.016.
- Penilla P.R., Bustos A.G., Elizalde S.G., 2006. Immobilization of Cs, Cd, Pb and Cr by synthetic zeolites from Spanish low-calcium coal fly ash. *Fuel*, 85, 823-32. DOI: 10.1016/j.fuel.2005.08.022.
- Rangel-Porrás G., Garcia-Magno J.B., Gonzalez-Munoz M.P., 2010. Lead and cadmium immobilization on calcitic limestone materials. *Desalination*, 262, 1-10. DOI: 10.1016/j.desal.2010.04.043.
- Reddy D.H.K., Seshaiha K., Reddy A.V.R., Madhava Rao M., Wang M.C., 2010. Biosorption of Pb<sup>2+</sup> from aqueous solutions by *Moringa oleifera* bark: equilibrium and kinetic studies. *J. Hazard. Mater.*, 174, 831-838. DOI: 10.1016/j.jhazmat.2009.09.128.
- Ruhl L., Vengosh A., Dwyer G.S., Hsu-Kim H., Deonarine A., 2010. Environmental Impacts of the Coal Ash Spill in Kingston, Tennessee: An 18-Month Survey. *Environ. Sci. Technol.*, 44, 9272-9278. DOI: 10.1021/es1026739.
- Scott M. A., Kathleen A.C., Prabir K.D., 2003. Handbook of zeolite science and technology, (Eds.), CRC Press, 16., USA, ISBN: 0824740203.
- Seredin V.V., Finkelman R.B., 2008. Metalliferous coals: A review of the main genetic and geochemical types. *Int. J. Coal Geol.*, 76, 253-289. DOI: 10.1016/j.coal.2008.07.016.
- Sočo E., Kalembkiewicz J., 2007. Investigations of sequential leaching behaviour of Cu and Zn from coal fly ash and their mobility in environmental conditions. *J. Hazard. Mater.*, 145, 482-487. DOI: 10.1016/j.jhazmat.2006.11.046.
- Sočo E., Kalembkiewicz J., 2009. Investigations on Cr mobility from coal fly ash. *Fuel*, 88, 1513-1519. DOI: 10.1016/j.fuel.2009.02.021.
- Kielland J., 1937. Individual activity coefficients of ions in aqueous solutions, *J. Am. Chem. Soc.*, 59, 1675-1678.
- Sočo E., Kalembkiewicz J., 2013. Adsorption of nickel(II) and copper(II) ions from aqueous solution by coal fly ash. *J. Environ. Chem. Eng.*, 1, 581-588. DOI: 10.1016/j.jece.2013.06.029.
- Visa M., Isac L., Duta A., 2012. Fly ash adsorbents for multi-cation wastewater treatment. *Appl. Surf. Sci.*, 258, 6345-6352. DOI: 10.1016/j.apsusc.2012.03.035.
- Weber T. W., Chakravorti , 1974. Pore and solid diffusion models for fixed-bed adsorbers. *AIChE J.*, 20, 228-238. DOI: 10.1002/aic.690200204.
- Weber W. J. Jr., Morris J. C., 1963. Kinetics of adsorption on carbon from solution. *J. Sanitary Eng. Div.*, 89, 31-60.
- Zhenga L., Danga Z., Yi X., Zhanga H., 2010. Equilibrium and kinetic studies of adsorption of Cd(II) from aqueous solution using modified corn stalk. *J. Hazard. Mater.*, 176, 650-656. DOI: 10.1016/j.jhazmat.2009.11.081.

Received 05 August 2014

Received in revised form 03 June 2015

Accepted 13 October 2015